Electronic Supplementary Material (ESI) for Journal of Materials Chemistry C.

Supporting Information

Sulfur-doping tuning oxygen vacancy in ultrathin 2D Ni-V mixed metal oxide for exceptional oxidase mimic and antibacterial application

Yi Wang[a,b], Chao Chen[a,b], Dun Zhang*[a,b]

[a]CAS Key Laboratory of Marine Environmental Corrosion and Bio-fouling, Institute of Oceanology, Chinese Academy of Sciences, 7 Nanhai Road, Qingdao 266071, China

[b]Open Studio for Marine Corrosion and Protection, Pilot National Laboratory for Marine Science and Technology (Qingdao), 1 Wenhai Road, Qingdao 266237, China

* Corresponding author: Dun Zhang (zhangdun@qdio.ac.cn)

1. Experimental

1.1. Materials

TMB, Live/Dead fluorescein, 2',7'-dichlorodihydrofluorescein diacetate (DCFH-DA) and 5,5,-dimethyl-1-pyrroline N-oxide (DMPO) were purchased from Sigma-Aldrich (Shanghai, China). $NiCl_2 \cdot 6H_2O$, VCl_3, urea, sulfur powder, H_2O_2 solution (30 wt% aqueous), and other chemicals were all of the analytical grades and obtained from Sinopharm Chemical Reagent Co., Ltd. (China). The aqueous solutions all were prepared with deionized water.

1.2. Preparation of S-doping Ni-V MMOs

The Ni-V LDH precursor was fabricated by the urea hydrolysis method. For Ni-V LDHs with a Ni/V molar ratio of 2:1, 4.8 mmol of $NiCl_2$ and 2.4 mmol of VCl_3 were dissolved into 70 mL of deionized water and then mixed with 10 mmol of urea under vigorous stirring. The mixed solution was transferred into a 100 mL Teflon-lined autoclave and maintained at 120 ^oC for 12 h. The precipitate was filtered and washed thoroughly with deionized water and absolute ethyl alcohol. The resulting solids were dried at 80 ^oC for 6 h. Ni-V LDHs with Ni/V molar ratios of 3:1 and 4:1 were synthesized using the same procedure. For the synthesis of the sulfur-doping Ni-V MMOs, 30 mg of Ni-V LDHs and 30 mg of sulfur powder were placed at two separate positions in a porcelain boat with sulfur at the upstream side of the tube furnace. Then, the porcelain boat was annealed at 400 ^oC for 2 h with a heating rate of 5 ^oC/min under an N_2 flow. Afterward, the furnace was cooled down to room temperature naturally. The corresponding materials were denoted as nNiV-S-400 (n=2, 3, and 4), respectively. For comparison, Ni-V MMOs were prepared [35].

1.3. Apparatus and characterization

X-ray diffractometer (XRD) patterns were performed on an Ultima IV X-ray

diffractometer (Rigaku, Japan) using Cu K_α radiation (λ=0.15418 nm) at 40 kV and 40 mA with the 2θ ranging from 5° to 80°. The morphological features of the samples were investigated by (SEM) images characterised on a Nova Nano SEM450 (FEI, America) and transmission electron microscopy (TEM) images captured on a JEM-2100 transmittance electron microscopy (JEOL, Japan). Following the image captured, Energy-dispersive X-ray spectroscopy (EDS) and mapping were performed. The Brunauer-Emmett-Teller (BET) test was measured on MicroActive for ASAP 2460 Version 2.01. Surface electronic states of the samples were tested by X-ray photoelectron spectroscopy (XPS) on an ESCALAB 250 X-ray photoelectron spectrometer (Thermo Fisher Scientifical Inc., USA) through an Al anode at a total power dissipation of 150 W (15 kV, 10 mA), and the banding energy was a reference to C 1s at 284.6 eV from adventitious carbon. Electron spin resonance (ESR) was measured using an EMX plus ESR spectrometer (Bruker, Germany) and the radical was trapped by DMPO.

1.4. Enzyme-like activity and mechanism

The enzyme-like activities of 2NiV-S-400 powders were measured by a standard TMB liquid substrate system with or without H_2O_2 at room temperature. Briefly, 90 μg/mL 2NiV-S-400 powders and 2 mM TMB with or without 10 mM H_2O_2 were put into 1 mL of NaAc-HAc buffer solution (pH 4). As the substrate TMB was added, the color changes can be immediately observed with the naked eye. The absorbance value of the mixed solution at 652 nm was recorded after 3 min reaction using an Infinite M1000Pro (Switzerland). To explore the effect of $\cdot O_2^-$ and ·OH active species restricting in catalytic reaction in the solution, 1 mM DMPO was implemented into the 2NiV-S-400-TMB system with other experimental conditions fixed to restrict the active

species.

1.5. Steady-state kinetic analysis

The dependence of the POD mimic catalytic activity of 2NiV-S-400 on pH and catalyst concentration was studied. pH 4 and the concentration (90 μg/mL) of catalyst were optimized to carry out the steady-state kinetic analysis experiments with varying concentrations of TMB at a fixed concentration of H_2O_2 or vice versa at room temperature. Absorbance values monitored at 652 nm for all reactions were back-converted to TMB concentration derived oxidation products by the Beer-Lambert Law, A=εbC; in which the molar absorption coefficient ε was 39000 $M^{-1}cm^{-1}$, path length b was 0.3237 cm. Kinetic parameters were fitted based on the Michaelis-Menten equation:

$$v_0 = v_{\max}\frac{[S]}{[S]+K_m}$$

where v_0 is the initial conversion rate, which can be calculated by the initial slope of absorbance changes with time, V_{max} is the maximum conversion rate, [S] is the substrate concentration, and K_m is the Michaelis constant. Lineweaver-Burk model $\frac{1}{v_0} = \frac{1}{v_{\max}} + \frac{K_m}{v_{\max}} \cdot \frac{1}{[S]}$ was also used to fit kinetic parameters.

1.6. Antibacterial activity

To inspect the bactericidal activity of 2NiV-S-400 based on OXD and POD mimic activity, *E. coli* as the representative of Gram-negative bacteria was used to study the bactericidal effect depended on the concentration of H_2O_2 and 2NiV-S-400, respectively. Monocolony of *E. coli* was incubated in a 5 mL liquid Luria–Bertani broth medium for cultural growth to the logarithmic phase. The obtained bacterial suspension (diluted to 10^6 CFU/mL) was mixed with various concentrations of H_2O_2 and 2NiV-S-400 for 2 h at room temperature. All the treated bacterial strains were diluted to 10^2 CFU/mL and incubated on an agar plate at 30 °C for 36 h before being calculated through standard

planting methods. To ensure the accuracy of the results, three parallel tests were performed. The bactericidal rate was calculated according to the equation: bactericidal rate (%)=(N_0-N_t)/N_0. N_0 was the number of coenobium for the blank team and N_t was the number of coenobium for the test team.

1.7. Measurement of intracellular $\cdot O_2^-$

To investigate the sterilization mechanism, the oxidant-sensitive dye DHE was used to assess the intracellular $\cdot O_2^-$ level. Briefly, after being treated with 2NiV-S-400 and H_2O_2, bacterial cells were cultivated with 10 μM DHE for another 30 min in the dark at room temperature. Before determined the intracellular $\cdot O_2^-$ radical and its level, bacterial cells were washed with phosphate buffer solution once. The stained bacterial was observed by OLYMPUS BX53M fluorescence microscopy.

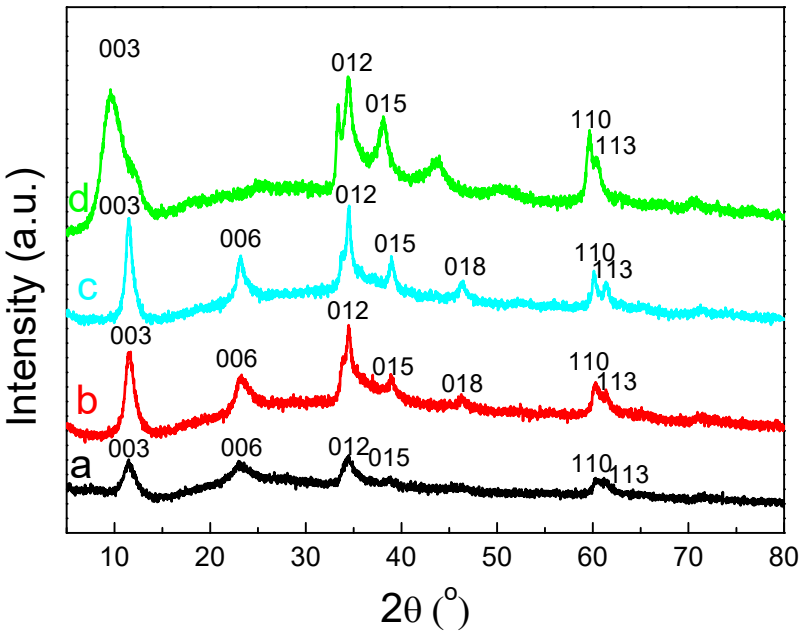

Fig. S1. XRD patterns of (a) 2NiV-LDHs, (b) 3NiV-LDHs, (c) 4NiV-LDHs, and (d) $Ni(OH)_2$.

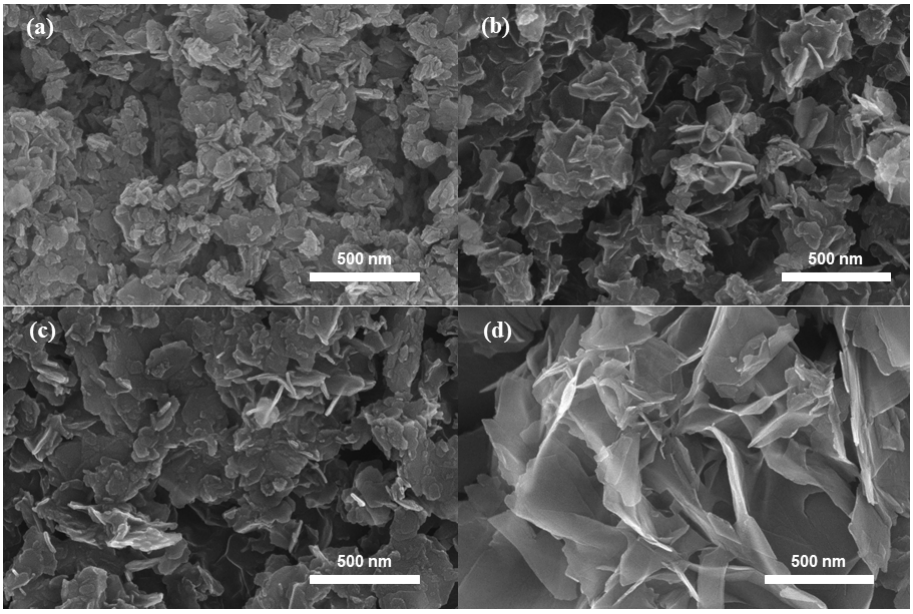

Fig. S2. SEM image of (a) 2NiV-LDHs, (b) 3NiV-LDHs, (c) 4NiV-LDHs, and (c) $Ni(OH)_2$.

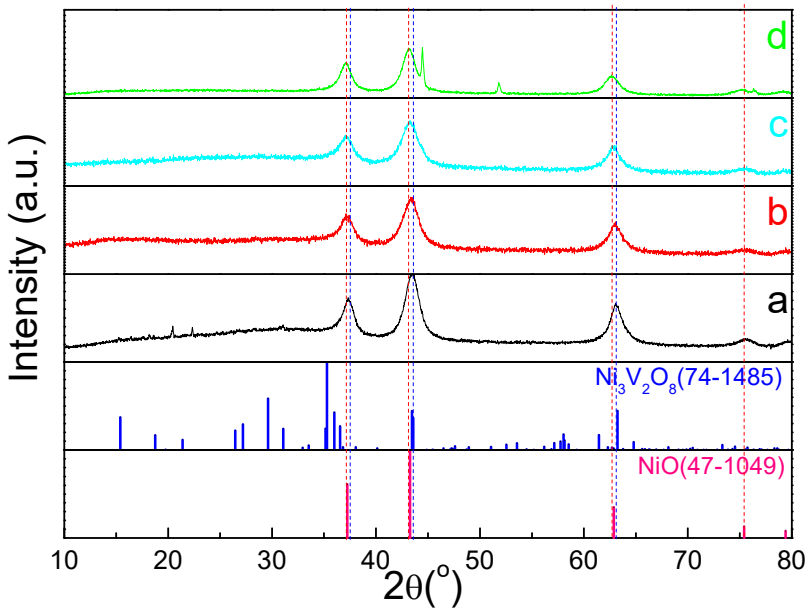

Fig. S3. XRD patterns of (a) 2NiV-S-400, (b) 3NiV-S-400, (c) 4NiV-S-400, and (c) Ni-S-400.

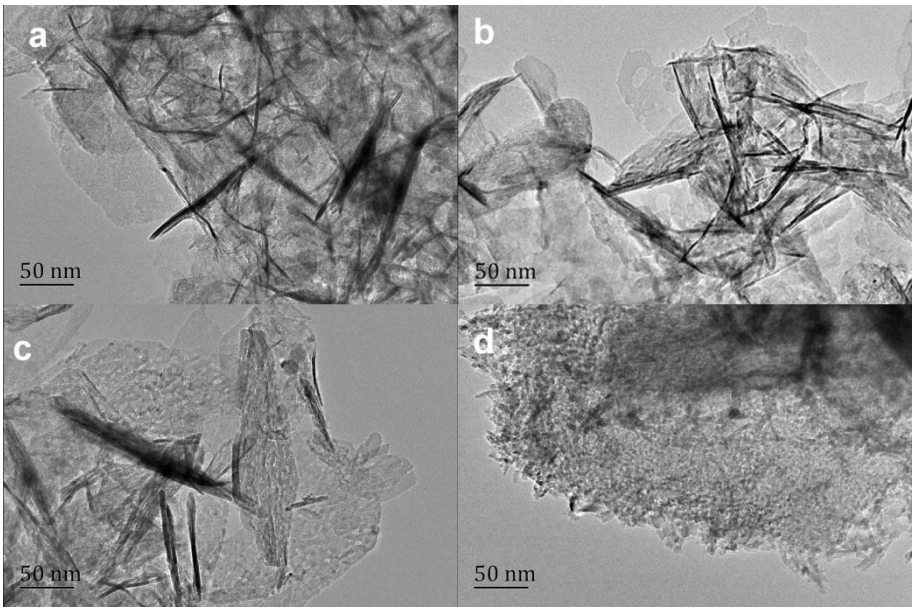

Fig. S4. TEM image of (a) 2NiV-S-400, (b) 3NiV-S-400, (c) 4NiV-S-400, and (c) Ni-S-400.

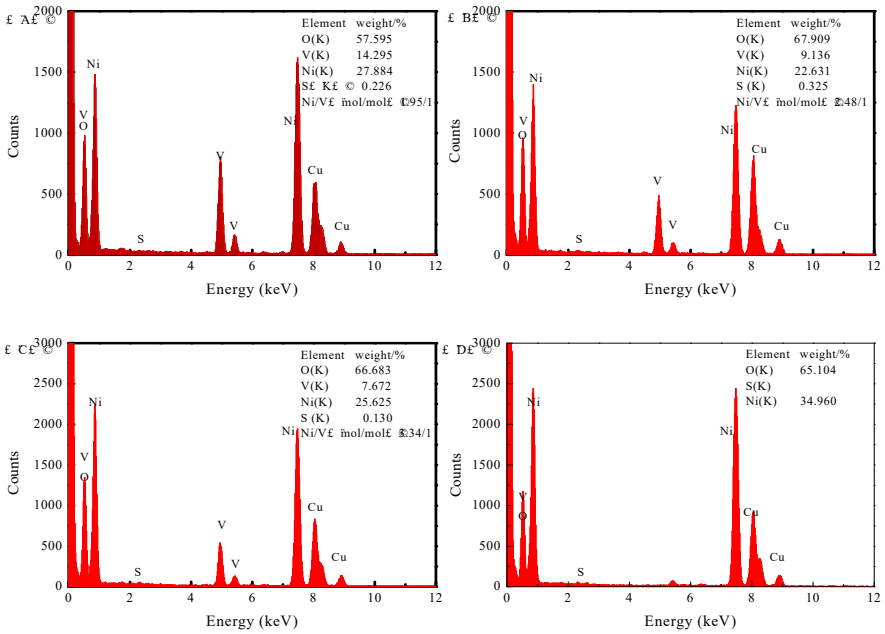

Fig. S5. EDS spectra of (A) 2NiV-S-400, (B) 3NiV-S-400, (C) 4NiV-S-400, and (D) Ni-S-400.

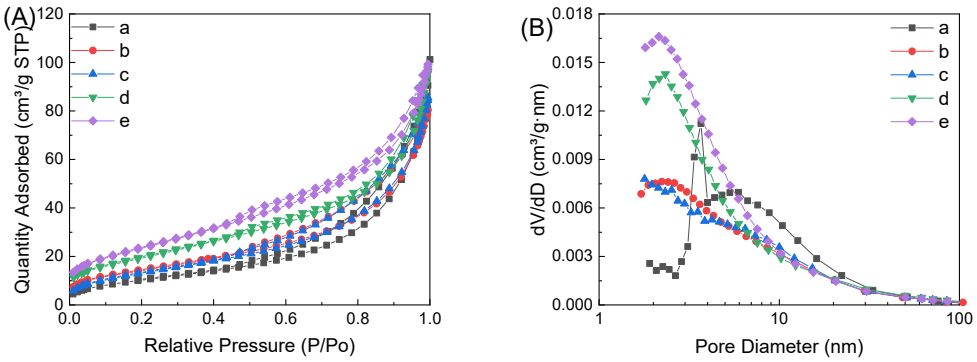

Fig. S6 N_2 adsorption-desorption isotherms of (a) 2NiV-S-400, (b) 3NiV-S-400, (c) 4NiV-S-400, (d) Ni-S-400 and (e) 2NiV-O-400

Table S1. Pore structure parameters of catalysts

Samples	Surface area(m^2 g^{-1})	Pore size (nm)	Pore volume (cm^3 g^{-1})
2NiV-S-400	38.09	13.57	0.13
3NiV-S-400	51.46	9.22	0.12
4NiV-S-400	49.04	10.15	0.12
Ni-S-400	70.04	8.07	0.14
2NiV-O-400	84.65	7.26	0.15

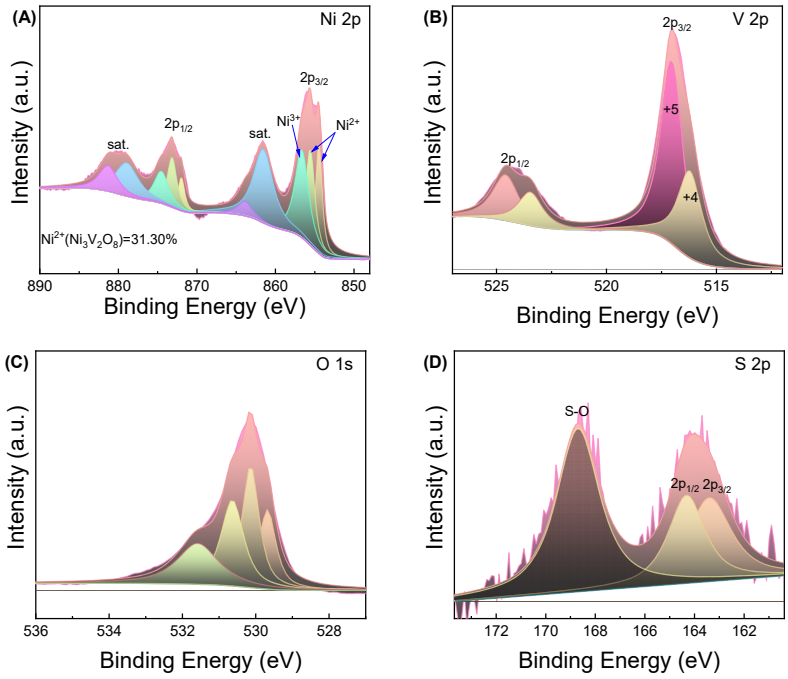

Fig. S7. XPS spectra of 3NiV-S-400 (A: Ni 2p; B: V 2p; C: O 1s; D: S 2p)

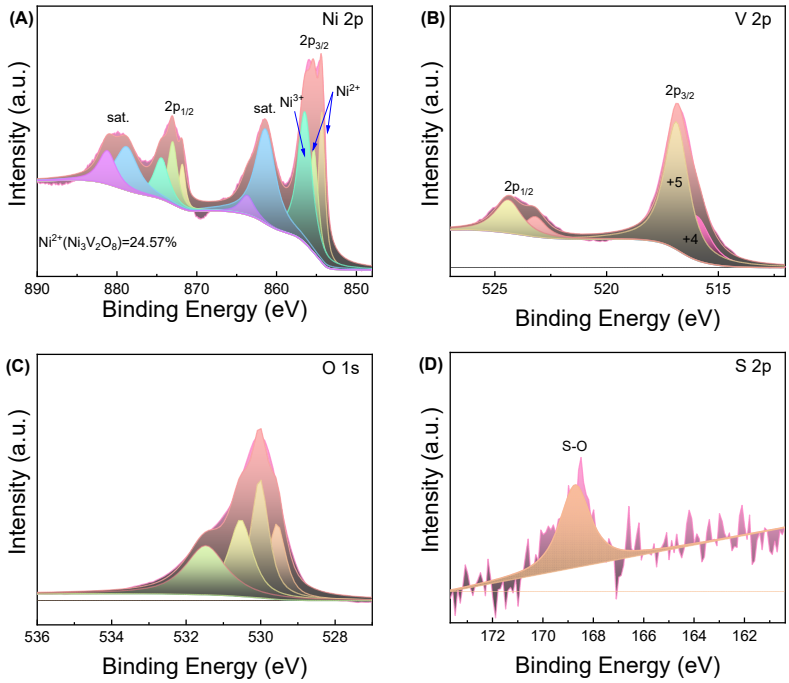

Fig. S8. XPS spectra of 4NiV-S-400 (A: Ni 2p; B: V 2p; C: O 1s; D: S 2p)

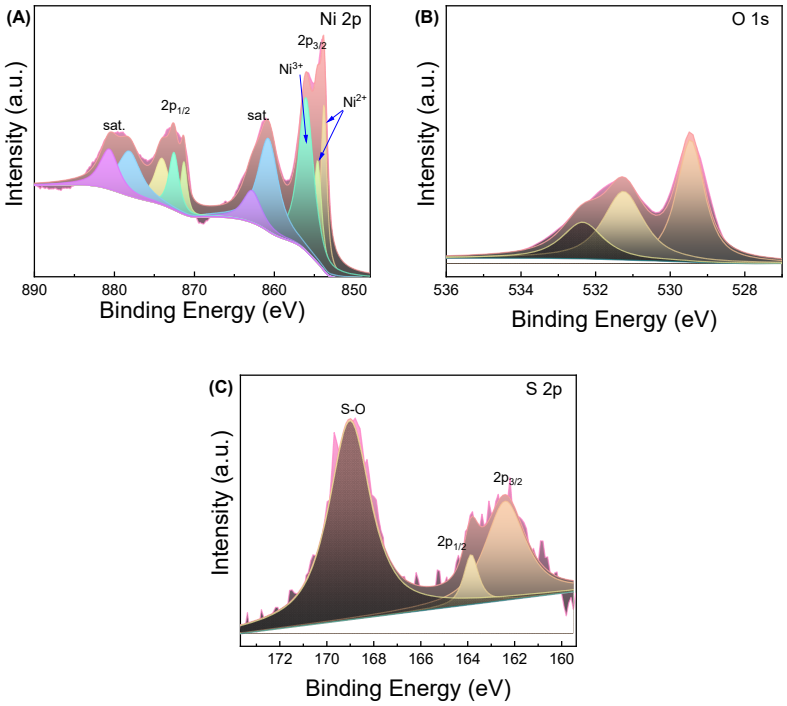

Fig. S9. XPS spectra of Ni-S-400(A: Ni 2p; B: V 2p; C: O 1s).

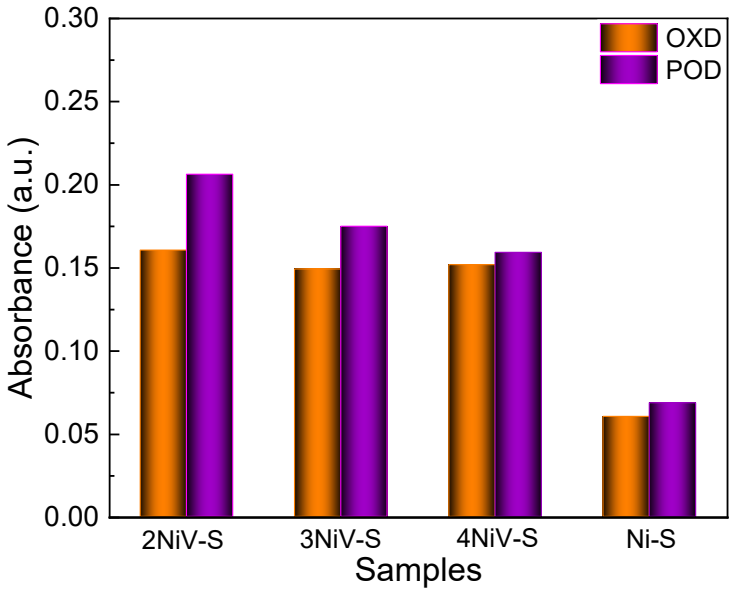

Fig. S10. POD and OXD catalytic activity of 2NiV-S-400, 3NiV-S-400, 4NiV-S-400, and Ni-S-400.

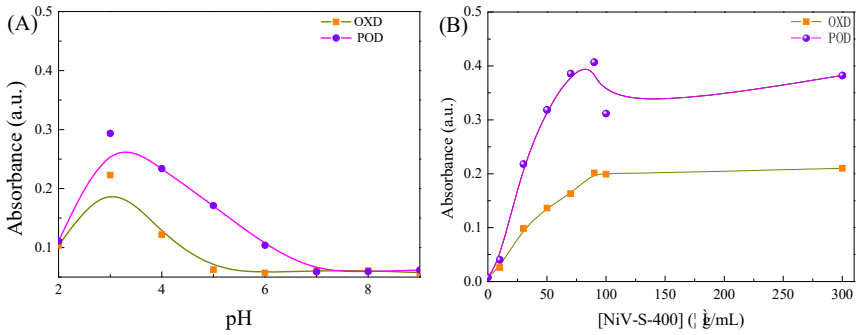

Fig. S11. (A) The optimizational experiment of pH and (B) the concentration of 2NiV-S-400 catalysts while the concentration of H_2O_2 and TMB were set as 0.8 mM and 0.2 mM, respectively

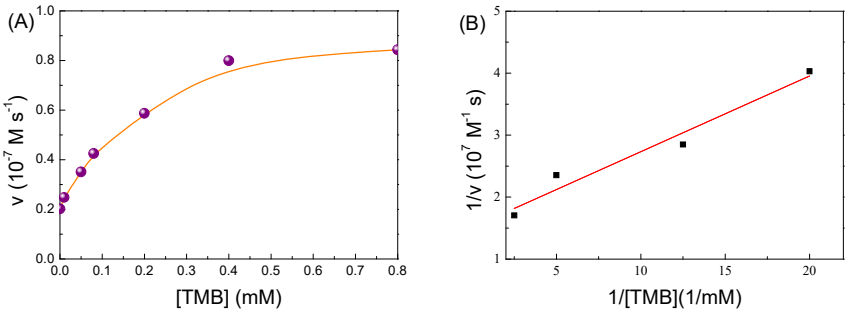

Fig. S12. Steady-state kinetic analysis and oxidase-like catalytic mechanism of 2NiV-S-400: (A) the TMB concentration was varied in the absence of H_2O_2; (B) Double reciprocal plots of activity of 2NiV-S-400 with the concentration of TMB varied.

Table S2 Michaelis - Menten constant (K_m) and maximum velocity (V_{max}) obtained from the double reciprocal plots which have been compared with other materials

	K_m [mM]		V_{max} [nM s^{-1}]		
	H_2O_2	TMB	H_2O_2	TMB	
2NiV-S-400	1.848	0.015	194.1	258.4	This work
NiV-MMO	15.000	0.437	20.2	31.4	[36]
HRP	3.700	0.434	87.1	100.0	[7]

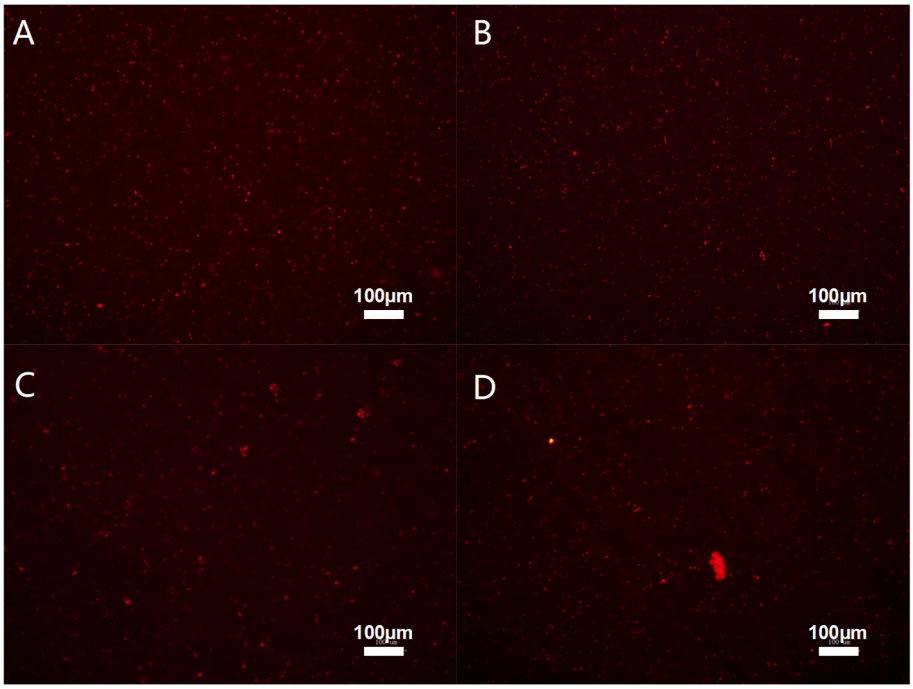

Fig. S13. Representative fluorescence images of $\cdot O_2^-$ levels in *E. coli* cells after different treatment (A: Blank; B: H_2O_2; C: 2NiV-S-400; D: H_2O_2+ 2NiV-S-400)